e-J. Surf. Sci. Nanotech. Vol. 12 (2014) 252-258 Conference - ACSIN-12&ICSPM21 -

Decoration of Titanate Nanowires and Nanotubes by Gold Nanoparticles: XPS, HRTEM and XRD Characterization*

J. Kiss†
Department of Physical Chemistry and Materials Science, University of Szeged, H-6720 Aradi vertanuk tere 1, Hungary, and MTA-SZTE Reaction Kinetics and Surface Chemistry Research Group, University of Szeged, H-6720 Rerrich B. 1, Hungary

P. Pusztai
Department of Applied and Environmental Chemistry, University of Szeged, H-6720 Rerrich B. 1, Hungary

L. Óvári
MTA-SZTE Reaction Kinetics and Surface Chemistry Research Group, University of Szeged, H-6720 Rerrich B. 1, Hungary

K. Baán, G. Merza, and A. Erdöhelyi
Department of Physical Chemistry and Materials Science, University of Szeged, H-6720 Aradi vertanuk tere 1, Hungary

A. Kukovecz
Department of Applied and Environmental Chemistry, and MTA-SZTE "Lendulet" Porous Nanocomposites Research Group, University of Szeged, H-6720 Rerrich B. 1, Hungary

Z. Kónya
Department of Applied and Environmental Chemistry, and MTA-SZTE Reaction Kinetics and Surface Chemistry Research Group, University of Szeged, H-6720 Rerrich B. 1, Hungary

(Received 9 December 2013; Accepted 24 March 2014; Published 31 May 2014)

Gold decorated titanate nanowires and nanotubes were investigated by XPS, XRD and HRTEM. XPS and UV-Vis diffuse reflectance results suggested that a certain part of gold underwent an ion exchange process. Higher gold loadings lead to the formation of nanosized-dispersed particles complexed to oxygen vacancies, with a diameter distribution of 1.5-10 nm. Gold additives catalyzed the transformation of the tube structure to anatase. Gold, however, stabilized the wire-like structure up to 873 K. [DOI: 10.1380/ejssnt.2014.252]

Keywords: Titanate nanowire; Titanate nanotube; Gold nanoparticles; X-ray photoelectron spectroscopy; Electron microscopy; X-ray diffraction

I. INTRODUCTION

Heterogeneous catalysts are key components in 21st century technology. Not only are most bulk and fine chemicals produced using heterogeneously catalyzed reaction steps, but suitable catalysts may also be the key ingredients in future energy production, energy storage and solving environmental problems [1–4]. Various tubular metal oxides have been developed recently and are of interest because they are expected to exhibit novel physical and chemical properties [5–11]. These nanomaterials are often applied as catalyst supports because they have a large specific surface area and may undergo an ion exchange process with metals [12–16]. High-aspect-ratio TiO_2 and titanate nanostructures are intensively studied at present because of their promising photoelectrical [17, 18] biomedical [19] and Li^+ and hydrogen storage properties [20–22]. TiO_2 structures are widely used in photochemical applications, whereas titanates offer excellent ion exchange properties [23], which are absent from rutile and anatase. Therefore, both TiO_2 and titanate nanostructures are promising materials from the heterogeneous catalytic point of view. Organic photovoltaics (OPVs) incorporated with TiO_2 nanowires show lower energy disorder, improved charge transport, more balanced electron-hole mobility and enhanced performance [24]. In addition, nanostructured titanates have impressive mechanical properties [25]. A comprehensive review [26] and a further work [27] about the fabrication, modification and application of titania nanoobjects were published recently.

Nanotubes and nanowires prepared either by the sol-gel method [7, 28, 29] or by hydrothermal conversion [10] can stabilize gold and rhodium in a dispersed form (1.5-5 nm) [29–31]. Palladium nanoclusters in different sizes could be also prepared on TiO_2 nanotube arrays [12], where the nanotubes were prepared by electrochemical

*This paper was presented at the 12th International Conference on Atomically Controlled Surfaces, Interfaces and Nanostructures (ACSIN-12) in conjunction with the 21st International Colloquium on Scanning Probe Microscopy (ICSPM21), Tsukuba International Congress Center, Tsukuba, Japan, November 4-8, 2013.

†Corresponding author: jkiss@chem.u-szeged.hu

methods [32, 33]. Gold-containing titania nanotubes were found to outperform the Degussa P-25 reference catalyst in the photo-oxidation of acetaldehyde [29], the water-gas shift reaction [34] and CO and hydrogen oxidation [28, 35]. Gold supported on titanate nanostructures (tubes and wires) exhibited significant catalytic activity in the hydrogenation of CO_2 [36] and in ethanol decomposition [37].

Since gold is the least reactive metal, it has been generally regarded as poorly active as a heterogeneous catalyst. However, when the gold is deposited on certain metal oxides (including TiO_2) as ultra-fine particles, its chemistry changes dramatically [3]. Understanding the nucleation and growth of metal on oxide surfaces is of critical importance in a wide variety of applications including heterogeneous catalysis [38–41]. The catalytic performance of gold markedly depends on the dispersion, the supports and the preparation method. When gold was deposited as hemispherical particles with a diameter smaller than 5 nm, it exhibited surprisingly high activities in the combustion of CO and saturated hydrocarbons [4, 42] as well as in the oxidation of methanol on $Au/TiO_2(110)$ [43]. Understanding the chemical environment and morphology of gold particles is extremely important. The growth, morphology and surface characterization of Au on $TiO_2(110)$ characterized by STM, XPS and LEIS were the subject of several recent works [44–55]. The main message of these studies is that the rate of diffusion, particle sizes and bonding energy of Au to $TiO_2(110)$ are markedly influenced by the structure of $TiO_2(110)$ surfaces. It was shown experimentally that the nucleation probability could be enhanced by forming additional surface defects. Consistent with this, Iddir and co-workers have shown in their theoretical work that there is a substantial difference in the bonding energies insofar as they are much higher at oxygen vacancies [56].

Titanate nanostructures are prepared by the alkali hydrothermal recrystallization of TiO_2 into sodium trititanate. Although the thermodynamically favored species under the reaction conditions is the nanowire, it is possible to exploit the slow kinetics of the recrystallization and stop the reaction at a point where the product mixture consists mostly of titanate nanotubes [10]. Nanotubes and nanowires are both constructured from a negatively charged framework of edge- and corner-sharing TiO_6 octahedra. The charge is compensated by mobile cations located in the interlayer ion exchange positions. Of course, compensating, easily exchangeable cations are not present in TiO_2. It is rather plausible that this structural difference between titanate nanostructures and TiO_2 can affect their interaction with metal atoms/ions. For this reason, in this work the interaction of Au with titanate nanowires/nanotubes and with $TiO_2(110)$ is characterized and compared. Beside the chemical state and bonding of Au to the support, the effect of Au on the thermal stability of titanate nanostructures is addressed, motivated by our previous work describing the destabilizing effect of rhodium on titanate nanowires and nanotubes [13].

II. EXPERIMENTAL

The titanate nanowires and nanotubes were prepared by mixing 2 g of anatase into 140 cm^3 10 M aqueous NaOH solution until a white suspension was obtained, aging the suspension in a closed, cylindrical, Teflon-lined autoclave at 400 K for 1-72 h while rotating the whole autoclave intensively at 60 rpm around its short axis, and finally washing the product with deionized water and neutralizing with 0.1 M HCl acid solution to reach pH=7; at this point, the titanate nanostructures slurry was filtered and dried in air at 353 K [10]. Acid washing is a standard method in titanate nanotube and nanowire synthesis. It is used to exchange as much Na^+ ions in the structure to protons as possible. The resulting material is generally referred to as "H-form" titanate. The benefits of this procedure are (i) that the material is converted into a quasi-standard form which can be readily reproduced in any laboratory, and (ii) that H-form titanates are more easily converted to β-TiO_2 or anatase thermally by water loss than their Na^+-containing counterparts. It should be noted that the integrity of the trititanate structure could be compromised below pH 7. The impurity level of the produced nanocomposites was less than 1%. The foreign elements determined by X-ray photoelectron spectroscopy (XPS) were C, Ca, and Na that remained in the product from the preparation process. The Au containing titanate nanowires and nanotubes samples with the same actual Au loading, 1-2.5% were prepared by deposition-preparation method [35–37] at pH=7 and at 343 K, followed by treatment in H_2 at 473 K.

The ultra high vacuum experiments were done in two separate chambers. One of them (1) was used to analyze the high area titanate samples, while measurements related to $TiO_2(110)$ were conducted in the other (2).
Chamber (1): XP spectra were taken with a SPECS instrument equipped with a PHOIBOS 150 MCD 9 hemispherical analyzer. The analyzer was operated in the FAT mode with 20 eV pass energy. The Al Kα radiation ($h\nu$ = 1486.6 eV) of a dual anode X-ray gun was used as an excitation source. The gun was operated at a power of 150 W (12.5 kV, 12 mA). The energy step was 25 meV, electrons were collected for 100 ms in one channel. Typically five scans were summed to get a single high-resolution spectrum. The Ti $2p_{3/2}$ maximum (458.9 eV) was used as the energy reference. The same data were obtained when C 1s (adventitious carbon at 285.1 eV), or O 1s lattice oxygen (530.4 eV) were used as references. The sample preparation chamber was directly connected to the measuring chamber to avoid the contamination of samples between the steps. For spectrum acquisition and evaluation both manufacturer's (SpecsLab2) and commercial (CasaXPS, Origin) software packages were used.
Chamber (2): Experiments related to the $TiO_2(110)$ single crystal were conducted in a separate UHV chamber [37, 57]. The crystal was a product of PI-KEM. Its temperature could be controlled between 150-1000 K. The sample was cleaned by applying cycles of Ar^+ ion sputtering (5 μA, 1.5 keV, 10 min) at 300 K and vacuum annealing at 930 K for 5 min. Au was deposited from an e-beam evaporator supplied by Oxford Applied Research. The chamber had facilities for Auger electron spectroscopy (AES), XPS and LEIS. Electrons were detected by a Leybold EA 10/100 hemispherical analyzer. An Al Kα anode was used as an X-ray source and the binding energy scale was referenced to the $4f_{7/2}$ peak of a thick Au layer set to 84.0 eV.

UV-Vis diffuse reflectance spectra were obtained relative to the reflectance of a standard ($BaSO_4$) using an UV/Vis spectrophotometer (OCEAN OPTICS, Typ.USB 2000) equipped with a diffuse reflectance sampling accessory. The samples were pressed into pellets of 2 g $BaSO_4$ and 50 mg of the titanate material.

The morphology of the pristine and Au modified titanate nanostructures was characterized by transmission electron microscopy (FEI Tecnai G^2 20 X-Twin; 200 kV operation voltage, ×180000 magnification, 125 pm/pixel resolution). X-ray diffractometry (Rigaku MiniFlexII; CuKα) and electron diffraction technique were used for crystal structure and crystallinity determinations. The Au particle size distribution was determined by image analysis of the HRTEM pictures using the ImageJ software. At least five representative images of equal magnification, taken at different spots of the TEM grid were first subjected to rolling ball background subtraction and contrast enhancement, then the diameter of the metal nanoparticles in the image was manually measured against the calibrated TEM scale bar. Each diameter distribution histogram was constructed from 200 individual nanoparticle diameters [13, 14].

III. RESULTS AND DISCUSSION

We first review the basic XPS characteristics of stoichiometric and reduced $TiO_2(110)$ surfaces at 300 K. The XP photoelectron spectrum of an annealed, stoichiometric $TiO_2(110)$ is shown in Fig. 1(A). The Ti 2p emissions were symmetric; Ti $2p_{3/2}$ appeared at 458.8 eV corresponding to Ti^{4+}. The noble gas ion sputtering made it possible to reduce the $TiO_2(110)$. The Ne^+ bombarded $TiO_2(110)$ surface showed significant broadening towards the lower binding energy side, attributed to the transformation of a part of Ti^{4+} ions to Ti^{3+} (457.1 eV) and Ti^{2+} (455.2 eV).

Gold was deposited onto the reference $TiO_2(110)$ surfaces in the UHV chamber (2). The deposition rate was calibrated with a quartz crystal microbalance incorporated into the UHV chamber. In some cases it was cross-checked by calculating the Au coverage from XPS peak areas. The two methods agreed with a precision of 10%. The Au $4f_{7/2}$ peak positions were measured as a function of Au coverage. The peak appeared at 84.3 eV at very low coverage (0.04 ML) on the stoichiometric $TiO_2(110)$ surface. The position of this emission shifted slightly to lower binding energy with increasing coverage (Fig. 1(B)). Above 1 ML coverage it was located at 84.0 eV which corresponds to the bulk position. The observed shift can be attributed to the finite size of the clusters combined with the insulating nature of the substrate, which results in a less efficient screening of the core hole formed in the photoemission process. This "final-state" effect depends on particle size, which in turn correlates with $4f_{7/2}$binding energy [47, 58].

On reduced $TiO_2(110)$ the binding energy shift from submonolayer to monolayer is larger (> 0.6 eV) than that of the stoichiometric surface as indicated by the Au $4f_{7/2}$ spectra recorded at different gold coverages (Fig. 1(C) and 1(D)). It was shown experimentally that the nucleation probability could be enhanced by increasing the number of surface defects. The deposited Au forms smaller size crystallites in higher density on the thermally reduced surface relative to the stoichiometric substrate [59]. The same effect was observed for $TiO_2(110)$ surface bombarded with low energy Ar ions [60]. The average particle diameter of gold changed from 2.0 to 3.5 nm when the gold was deposited at 300 K on nearly perfect $TiO_2(110)$ [44–55, 61].

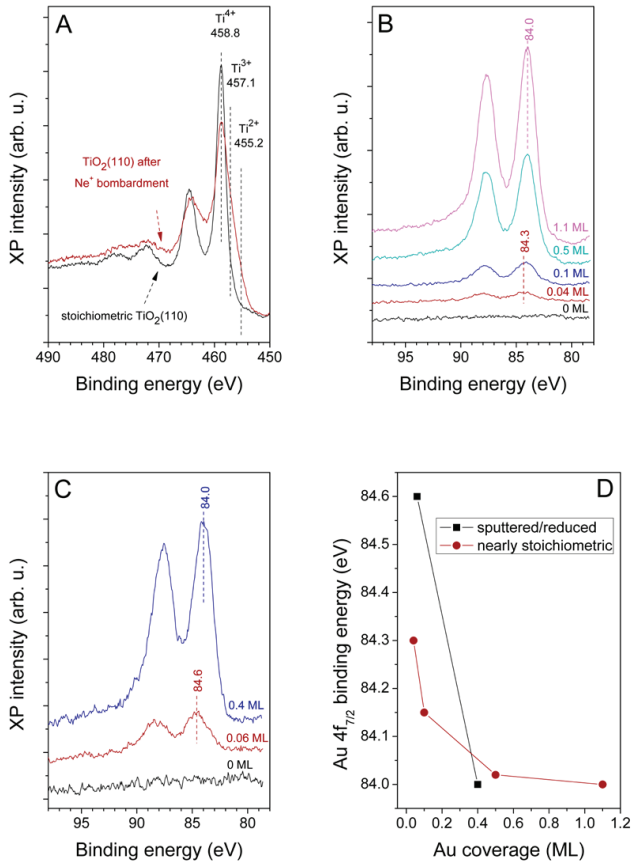

FIG. 1: The Ti 2p region of the nearly stoichiometric $TiO_2(110)$ surface and after Ne^+ bombardment (A); The Au 4f region collected after the evaporation of an increasing amount of Au at 300 K on a nearly stoichiometric $TiO_2(110)$ (B) and on the Ne^+ sputtered titania surface (C); The Au $4f_{7/2}$ peak positions as a function of Au coverage on the stoichiometric and on the sputtered $TiO_2(110)$ surface (D).

We now turn our attention to the properties of gold deposited on titanate nanotubes and nanowires. Atomically dispersed gold can be produced on porous TiO_2 and titania nanostructures (nanotubes, nanowires) by coprecipitation or deposition-precipitation methods [28–31, 35]. Although it is virtually impossible to prepare a truly monodisperse collection of metallic particles (i.e. particles of exactly the same diameter), in the past years significant progress was made in the preparation of gold particles with a narrow diameter distribution between ∼2-10 nm [28–31, 35, 42]. Using the above-mentioned preparation method, we produced gold nanoparticles on titanate nanowires and nanotubes. Figure 2 shows a typical HRTEM image obtained on nanowires and nanotubes. The size of Au nanoparticles is between 1.5 and 10 nm. The chemical environment of gold nanoparticles was characterized by XPS after reduction in H_2 atmosphere for 60 min at 473 K. The 4f spectra of gold deposited on

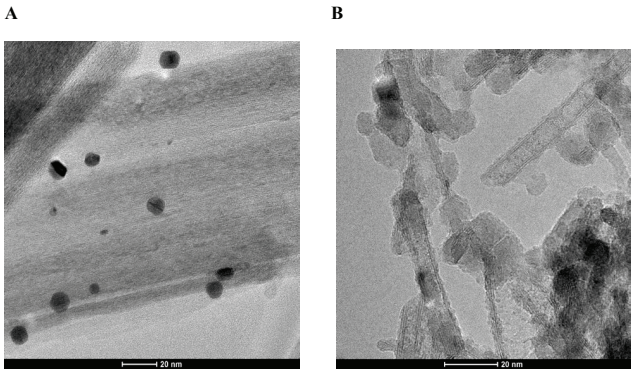

FIG. 2: HRTEM image on Au decorated (2.5%) titanate nanowires (A) and nanotubes (B).

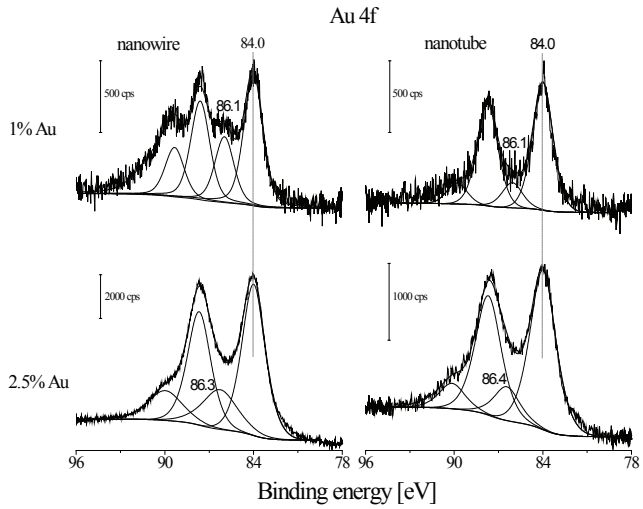

FIG. 3: Au $4f$ XPS on Au loaded titanate nanowires and nanotubes at different gold content.

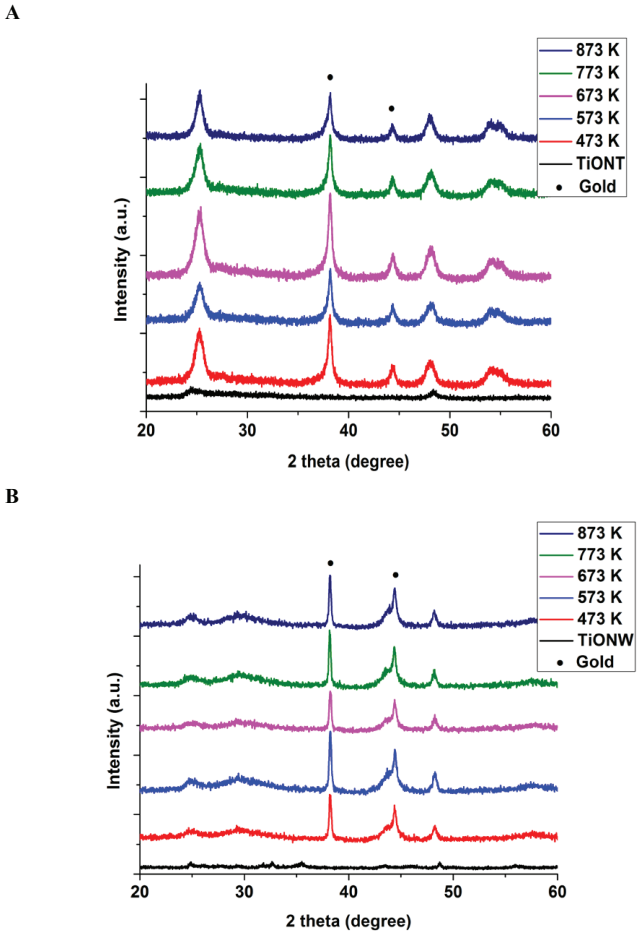

FIG. 4: XRD of Au loaded (2.5%) nanotubes (A) and nanowires (B) as a function of annealing temperature. The bottom diffractograms represent the pristine H-form titanate nanotubes and nanowires.

titanate nanostructures at two different Au loadings are displayed in Fig. 3. The observed features are quite different from those observed on $TiO_2(110)$ insofar as two peaks are present in the reduced sample spectra for Au $4f_{7/2}$ at 84.0 eV (metallic state) and at 86.1-86.4 eV.

Two different explanations can be offered for the appearance of this unusually high binding energy gold state. As mentioned above, core level shifts due to particle size must be considered in the interpretation of the spectra of nanoparticles [58]. Although this effect undoubtedly plays a role in the present case, the observed nearly 2 eV binding energy shift cannot be explained satisfactorily by this way alone. The second possible explanation is that Au may have undergone an ion exchange process. This is not possible on $TiO_2(110)$ because of the lack of compensating cations, however, it is quite likely to happen on titanates which are well-known for their ion-exchange ability [23].

An XPS-independent proof for the ion exchange can be obtained by measuring the band gap energy. Cheng *et al.* have provided theoretical evidence for ion exchange induced band gap reduction in a similar system (Ni-manganite) [62]. In our experimental work the band gap energy (E_g) was calculated according to Beranek and Kisch [63] who used the equation $\alpha = A(h\nu - E_g)^n/h\nu$, where α is the absorption coefficient, A is a constant, $h\nu$ is the energy of light and n is a constant depending on the nature of the electron transition. Assuming an indirect band gap ($n = 2$) for TiO_2 [64], with α proportional to $F(R_\infty)$ the band gap energy can be obtained from Kubelka-Munk plots (not shown) of $[F(R_\infty)/h\nu]^{1/2}$ vs. $h\nu$ as the interception at $[F(R_\infty)/h\nu]^{1/2} = 0$ of the extrapolated linear part of the plot. The band gap for pure titanate nanowire was 3.14 eV, while that for Au-doped titanate nanowire was less: 2.84 eV for 1 wt% and 2.50 eV for 2.5 wt% Au content. Somewhat smaller decreases in band gap energy were measured for gold containing nanotubes. The pronounced decrease of the band gap of titanate nanowires upon loading with Au suggests a very strong electronic interaction between the titanate nanostructure framework and gold, which may eventually result in an ion exchange process similar to that occurring in cobalt and silver loaded titanates [14, 16].

The temperature-induced transformation of titanate nanostructures into titania is intensely researched today. Of particular importance are studies on converting metal ion exchanged titanates into anatase, because this method

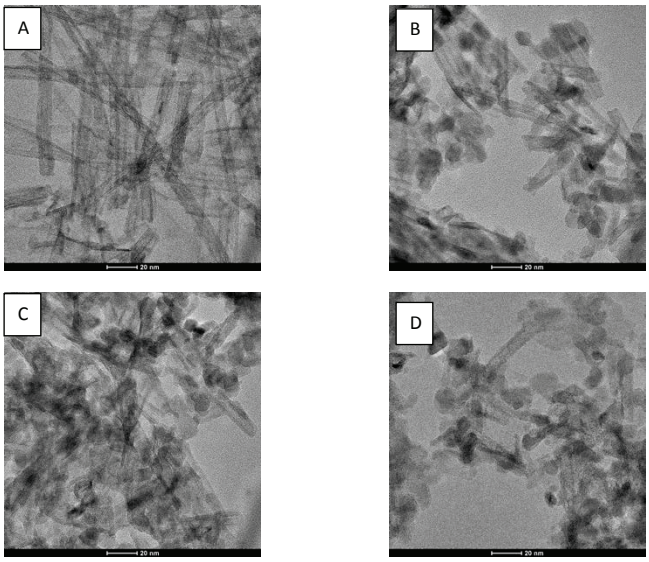

FIG. 5: HRTEM images of H-form titanate nanotubes (A) and Au containing (2.5%) nanotubes after different heat treatments; B – 473 K, C – 673 K, D – 873 K. The scale bars shown in A to D correspond to 20 nm.

offers excellent homogeneous metal doping [65]. Below we explore the behavior of gold-loaded titanate nanotubes upon thermal annealing. Acid washing resulted in a mild destruction of the inner and outer walls of the nanotubes (bottom diffractogram in Fig. 4(A)). According to previous studies thermal treatment below 673 K had no significant effect on the crystal structure [13]. Interestingly, typical anatase reflexions (25.3° (1 0 1), 37.0° (1 0 3), 37.8° (0 0 4), 38.6° (1 1 2), 48.1° (2 0 0), 53.9° (1 0 5)) appeared already at 473 K in gold-loaded samples in addition to the reflexions of gold (Fig. 4(A)). TEM images confirmed the tubular morphology of the as-synthesized titanate nanotubes with a diameter of ∼7 nm and length up to 80 nm. Partial wall destruction caused by acid washing is observable in Fig. 5(A). In agreement with the XRD results no morphological degradation could be observed without gold loading upon heat treatment up to 573 K (not shown). However, when the titanate nanotubes were decorated by gold, the tube structure was destroyed as low as at 473 K; the morphology did not change further up to 878 K (Fig. 5(B)-(D)).

Interestingly, gold-loaded titanate nanowires exhibit a somewhat different thermal behavior than nanotubes. The crystal structure of the pristine nanowires is a mixture of different titanate forms, mostly β-TiO_2 and $H_xNa_{(2-x)}Ti_3O_7$ as shown by several authors using X-ray diffractometry [10, 13, 14]. Acidic treatment also resulted in crystallinity degradation (bottom diffractogram in Fig. 4(B)). The crystal transformation is continuous during the thermal annealing process. XRD patterns recorded from a sample annealed at 473 and 573 K indicated the collapse of the layered structure and appearance of an anatase phase with low crystallinity. The presence of Rh and Co additives has been shown to accelerate this transformation [13, 14]. Therefore, it is a new and important observation of the present report that Au loading has not promoted this process; on the contrary, it stabilized the layered structure (Fig. 4(B)). The morphology of the titanate nanowire is unchanged up to 873 K. XRD showed reflections due to gold (38.2° (1 1 1), 44.4° (2 0 0)) at different temperatures. In agreement with the XRD results, the HRTEM images have also shown that nanowires preserve their wire-like morphology up to 873 K (Fig. 6).

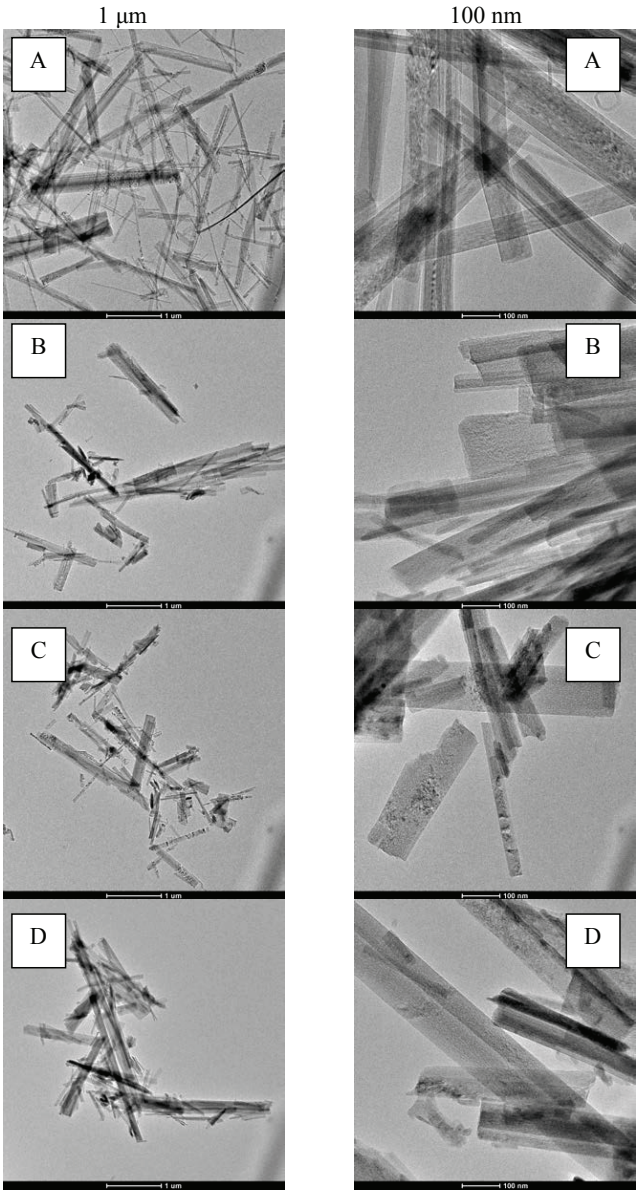

FIG. 6: HRTEM images of H-form titanate nanowires (A) and Au containing (2.5%) nanowires after different heat treatments; B – 473 K, C – 673 K, D – 873 K.

IV. CONCLUSIONS

Gold nanoparticles were prepared on one dimensional H-form titanate nanostructures as well as reference TiO_2(110) surfaces. The chemical nature and the morphology of gold particles were characterized by X-ray photoelectron spectroscopy, XRD and HRTEM. An unexpectedly high binding energy gold state was found by XPS in gold-loaded titanate nanostructures. This state

was absent from the spectra of gold-loaded TiO_2(110). A likely explanation for this phenomenon, supported also by characteristic decrease of band gap energy from 3.14 eV to 2.50 eV with increasing Au content, is that the depending on metal loading, Au is stabilized on titanate nanowires partially in positively charged gold form by ion exchange and also as Au clusters. Our second important new finding is that the thermal annealing behavior of Au loaded titanate nanotubes and nanowires are different. The former loose their tubular morphology and are readily transformed into anatase even at the very low temperature of 473 K. On the other hand, gold stabilizes the layered structure of titanate nanowires up to 873 K.

Acknowledgments

The financial support of TÁMOP-4.2.2.A-11/1/KONV-2012-0047, TÁMOP-4.2.2.A-11/1/KONV-2012-0060 and OTKA NN 110676 and the experimental works of Ms. E. Varga (XPS) and Mr. L. Nagy (XRD) are greatly acknowledged.

[1] G. Ertl, H. Knözinger, and J. Weitkamp, *Handbook of Heterogeneous Catalysis* (VCH, Weinheim, 1997), p. 5.
[2] G. Centi and S. Perathoner, Top. Catal. **52**, 948 (2009).
[3] M. Haruta, N. Yamada, T. Kobayashi, and S. Iijima, J. Catal. **115**, 301 (1989).
[4] M. Haruta, Catal. Today **36**, 153 (1997), and references therein.
[5] B. C. Satishkumar, A. Govindaraj, E. M. Vogl, L. Basumallick, and C. N. R. Rao, J. Mater. Res. **12**, 604 (1977).
[6] P. Hoyer, Langmuir **12**, 1441 (1996).
[7] T. Kasuga, M. Hiramatsu, A. Hoson, T. Sekino, and K. Niihara, Langmuir **14**, 3160 (1998).
[8] G. H. Du, Q. Chen, R. C. Che, Z. Y. Yuan, and L. M. Peng, Appl. Phys. Lett. **79**, 3702 (2001).
[9] D. S. Seo, J. K. Lee, and H. Kim, J. Cryst. Growth **229**, 428 (2001).
[10] E. Horváth, Á. Kukovecz, Z. Kónya and I. Kiricsi, Chem. Mater. **19**, 927 (2007).
[11] Y. Xu, Q. Yi, F. Yi, and L.-X. Yuan, Physics, Mechanics and Astronomy **55**, 14 (2012).
[12] A. Honciuc, M. Laurin, S. Albu, M. Sobota, P. Schmuki, and J. Libuda, Langmuir **26**, 14014 (2010).
[13] G. Pótári, D. Madarász, L. Nagy, B. László, A. Sápi, A. Oszkó, A. Kukovecz, A. Erdöhelyi, Z. Kónya, and J. Kiss, Langmuir **29**, 3061 (2013).
[14] D. Madarász, G. Pótári, A. Sápi, B. László, C. Csudai, A. Oszkó, A. Kukovecz, A. Erdöhelyi, Z. Kónya, and J. Kiss, Phys. Chem. Chem. Phys. **15**, 15917 (2013).
[15] X. Sun and Y. Li, Chem. Eur. J. **9**, 2229 (2003).
[16] F. Cesano, S. Bertarione, M. J. Uddin, G. Agostini, D. Scarano, and A. Zeccina, J. Phys. Chem. C **114**, 169 (2010).
[17] M. Hodos, E. Horváth, H. Haspel, Á. Kukovecz, Z. Kónya, and I. Kiricsi, Chem. Phys. Lett. **399**, 512 (2004).
[18] G. K. Mor, K. Shankar, M. Paulose, O. K. Varghese, and C. A. Grimes, Nano Lett. **5**, 191 (2005).
[19] S. Kubota, K. Johkura, K. Asanuma, Y. Okouchi, N. Ogiwara, K. Sasaki, and T. Kasuga, J. Mater. Sci.: Mater. Med. **15**, 1031 (2004).
[20] L. Kavan, M. Kalbac, M. Zukalova, I. Exnar, V. Lorenzen, R. Nesper, and M. Graetzel, Chem. Mater. **16**, 477 (2004).
[21] D. Baviykin, A. A. Lapkin, P. K. Plucinski, J. M. Friderich, and F. C. Walsh, J. Phys. Chem. B **109**, 19422 (2005).
[22] R. Huang, F. Chung, and E. M. Kelder, J. Electrochem. Soc. **153**, A1459 (2006).
[23] D. Madarász, I. Szenti, A. Sápi, J. Halász, Á. Kukovecz, and Z. Kónya, Chem. Phys. Lett. **591**, 161 (2014).
[24] P. Yang, D. K. Zhong, M. Yuan, A. H. Rice, D. R. Gamelin, and C. K. Luscombe, Phys. Chem. Chem. Phys. **15**, 4566 (2013).
[25] M. T. Byrne, J. M. McCarty, M. Bent, R. Blake, Y. K. Gun'ko, E. Horváth, Z. Kónya, Á. Kukovecz, I. Kiricsi, and J. N. Coleman, J. Mater. Chem. **17**, 2351 (2007).
[26] H.-H. Ou and S.-L, Lo, Sep. Purif. Technol. **58**, 179 (2007).
[27] L. Torrente-Murciano, A. A. Lapkin, and D. Chadwick, J. Mater. Chem. **20**, 6484 (2010).
[28] T. Akita, M. Okumura, K. Tanaka, K. Okhuma, M. Kohyama, T. Koyanagi, M. Data, S. Tsubota, and M. Haruta, Surf. Interface Anal. **37**, 265 (2005).
[29] S. S. Malwadkar, R. S. Gholap, S. V. Awante, P. Korake, M. G. Chaskar, and N. M. Gupta, **203**, 24 (2009).
[30] Á. Kukovecz, G. Pótári, A. Oszkó, Z. Kónya, A. Erdöhelyi, and J. Kiss, Surf. Sci. **605**, 1048 (2011).
[31] A. Oszkó, G. Pótári, A. Erdöhelyi, Á. Kukovecz, Z. Kónya, I. Kiricsi, and J. Kiss, Vacuum **85**, 1114 (2011).
[32] A. Ghicov and P. Schmuki, Chem. Commun. **20**, 2794 (2009).
[33] S. Bauer, S. Kleber, and P. Schmuki, Electrochem. Commun. **8**, 1321 (2006).
[34] V. Idakiev, Z.-Y. Yuan, T. Tabakova, and B.-L. Su, Applied Catal. A **281**, 149 (2005).
[35] M. Méndez-Cruz, J. Ramirez-Solis, and R. Zanella, Catal. Today **166**, 172 (2011).
[36] M. Tóth, J. Kiss, A. Oszkó, G. Pótári, B. László, and A. Erdöhelyi, Top. Catal. **55**, 747 (2012).
[37] J. Kiss, L. Óvári, A. Oszkó, G. Pótári, M. Tóth, K. Baán, and A. Erdöhelyi, Catal. Today **181**, 163 (2012).
[38] C. T. Campbell, Surf. Sci. Rep. **27**, 1 (1997).
[39] U. Diebold, Surf. Sci. Rep. **48**, 53 (2003).
[40] M. Bäumer and H. J. Freund, Prog. Surf. Sci. **61**, 127 (1999).
[41] Q. Fu and T. Wagner, Surf. Sci. Rep. **62**, 431 (2007).
[42] F. Boccuzzi, A. Chiorino, M. Manzoli, P. Lu, T. Akita, S. Ichikawa, and M. Haruta, J. Catal. **202**, 256 (2001).
[43] S. A. Tenny, B. C. Cagg, M. S. Levine, W. He, K. Manandhar, and D. A. Chen, Surf. Sci. **606**, 1233 (2012).
[44] L. Zhang, R. Persaud, and T. E. Madey, Phys. Rev. B **56**, 10549 (1997).
[45] Y. Maeda, T. Fujitani, S. Tsubota, and M. Haruta, Surf. Sci. **562**, 1 (2004).
[46] F. Consandey, T. E. Madey, Surf. Rev. Lett. **8**, 73 (2001), and references therein.
[47] C. Fan, T. Wu, and S. L. Anderson, Surf. Sci. **578**, 5 (2005).
[48] L. Bugyi, A. Berkó, L. Óvári, A. M. Kiss, and J. Kiss, Surf. Sci. **602**, 1650 (2008).
[49] L. Óvári, L. Bugyi, Zs. Majzik, A. Berkó, and J. Kiss, J. Phys. Chem. C **112**, 18011 (2008).
[50] J. B. Park, S. F. Conner, and D. A. Chen, J. Phys. Chem.

C **63**, 5490 (2008).
[51] L. Óvári, A. Berkó, N. Balázs, Zs. Majzik, and J. Kiss, Langmuir **26**, 2167 (2010).
[52] F. Gao, Y. Wang, D. W. Goodman, J. Phys. Chem. C **114**, 4036 (2010).
[53] H. L. Abbott, A. Aumer, Y. Lei, C. Asokan, R. J. Meyer, M. Sterrer, S. Shaikhutdinov, and H.-J. Freund, J. Phys. Chem. C **114**, 17099 (2010).
[54] S. A. Tenny, J. S. Ratliff, C. C. Roberts, W. He, S. C. Ammal, A. Heyden, and D. A. Chen, J. Phys. Chem. C **114**, 21652 (2010).
[55] R. P. Galhenage, H. Yan, S. A. Tenny, N. Park, G. Henkelman, P. Albrecht, D. Mullin, and D. A. Chen, J. Phys. Chem. C **117**, 7191 (2013).
[56] H. Iddir, S. Ögüt, N. D. Browning, and M. M. Disko, Phys. Rev. B **76**, 8 (2005).
[57] L. Óvári and J. Kiss, Appl. Surf. Sci. **252**, 8624 (2006).
[58] C. R. Henry, Surf. Sci. Rep. **31**, 231 (1988).
[59] B. K. Min, W. T. Wallace, and D. W. Goodman, Surf. Sci. **600**, L7 (2006).
[60] A. M. Kiss, M. Svec, and A. Berkó, Surf. Sci. **600**, 3352 (2006).
[61] K. Dumbuya, G. Cabailh, R. Lazzari, J. Jupille, L. Ringel, M. Pistor, O. Lytken, H.-P. Steinruck, and J. M. Gottfried, Catal. Today **181**, 20 (2012).
[62] J. R. Huang, H. Hsu, C. Cheng, J Magn. Magn. Mater. **358-359**, 149 (2014).
[63] R. Beranek and H. Kisch, Photochem. Photobiol. Sci. **7**, 40 (2008).
[64] H. Tang, K. Prasad, R. Sanilines, P. E. Schmid, and F. Lewy, J. Appl. Phys. **75**, 2042 (1994).
[65] P. Szirmai, E. Horváth, B. Nafradi, Z. Mickovic, R. Smajda, D. M. Djokic, K. Schenk, L. Forró, and A. Magrez, J. Phys. Chem. C. **117**, 697 (2013).